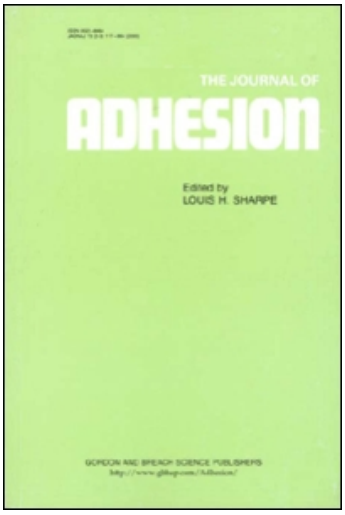

The Journal of Adhesion
Publication details, including instructions for authors and subscription information:
http://www.informaworld.com/smpp/title~content=t713453635

EXPERIMENTS AND INELASTIC ANALYSIS OF THE LOOP TACK TEST FOR PRESSURE-SENSITIVE ADHESIVES

Youngjin Woo[a]; Raymond H. Plaut[a]; David A. Dillard[a]; Stacy L. Coulthard[a]
[a] Center for Adhesive and Sealant Science, Blacksburg, Virginia, USA

Online publication date: 18 June 2010

To cite this Article Woo, Youngjin , Plaut, Raymond H. , Dillard, David A. and Coulthard, Stacy L.(2004) 'EXPERIMENTS AND INELASTIC ANALYSIS OF THE LOOP TACK TEST FOR PRESSURE-SENSITIVE ADHESIVES', The Journal of Adhesion, 80: 3, 203 — 221
To link to this Article: DOI: 10.1080/00218460490279251
URL: http://dx.doi.org/10.1080/00218460490279251

The Journal of Adhesion, 80: 203–221, 2004

ISSN: 0021-8464 print/1545-5823 online
DOI: 10.1080/00218460490279251

Taylor & Francis
Taylor & Francis Group

EXPERIMENTS AND INELASTIC ANALYSIS OF THE LOOP TACK TEST FOR PRESSURE-SENSITIVE ADHESIVES

Youngjin Woo
Raymond H. Plaut
David A. Dillard
Stacy L. Coulthard
Center for Adhesive and Sealant Science,
Virginia Polytechnic Institute and State University,
Blacksburg, Virginia, USA

The loop tack test is studied experimentally and numerically using a model system. The ends of a steel strip are clamped together, giving a teardrop shape, and the loop is pushed downward onto an acrylic foam tape and then pulled upward off the tape. In the finite element analysis, the strip is represented by beam elements and a bilinear elastic–plastic constitutive law. The traction–separation relationship for the pressure-sensitive adhesive (PSA) is modeled with a trapezoidal cohesive zone. Viscoelastic behavior of the PSA is included in one case. Curves of the pulling force versus *the top displacement (i.e., tack curves) exhibit a sharp peak just before separation of the loop from the strip. The effects of the PSA parameters, contact length, loop length and thickness, and loading rate are investigated. The numerical results compare more favorably with the experimental results than do those from a previous elastic analysis.*

Keywords: Loop tack; Pressure sensitive adhesive; Finite element analysis; Elastic foundation; Viscoelastic foundation

Received 8 August 2003; in final form 11 November 2003.

This research was supported by the National Science Foundation under Grant No. CMS-9713949 and by a fellowship from the Adhesion and Sealant Council Education Foundation provided through the Center for Adhesive and Sealant Science at Virginia Tech. The authors thank the reviewers for their helpful comments.

Address correspondence to Raymond H. Plaut, Department of Civil and Environmental Engineering, Virginia Tech, Mail Code 0105, Blacksburg, VA 24061, USA. E-mail: rplaut@vt.edu

INTRODUCTION

Adhesive tapes consisting of a backing and a pressure-sensitive adhesive (PSA) on one side are used in many applications [1]. PSA performance is often characterized by a range of tests that may generally be categorized by tack, static shear, or peel configurations. Tack, defined by the ability of a PSA to resist removal after brief application of a light pressure, is quantified by several techniques.

One method for determining the tack of an adhesive tape is the loop tack test. The ends of a strip of tape are folded upward to form a teardrop shape with the adhesive on the outside. Next, the top of the loop, with the ends clamped together, is pushed downward onto a rigid horizontal substrate, and then is pulled upward until the loop detaches from the substrate. The curve of the force *versus* the vertical displacement of the top of the loop is called the tack curve. In a modified form of the test, the adhesive is on the substrate rather than the loop. This modified test is considered here. Some experiments are performed, and a finite element model is developed to replicate the experimental results.

The loop tack test has been discussed by many researchers [2–14]. Several standard test methods exist [5, 6, 8], and some test results have been reported. Lin [3] listed the maximum detachment force (*i.e.,* tack force) for several peroxide-cured silicone PSAs on four substrates. Tack forces obtained using FINAT Test Method No. 9 were presented in [6–9, 11]. In these tests, the loop was 25.4 mm wide and approximately 155 mm long, the contact length on a glass or steel substrate was 25.4 mm, and the rate of loading and separation was 300 mm/min. One tack curve was shown [6], and it exhibited a short plateau and then a sharp peak before detachment from the substrate occurred.

Le *et al.* [10] reported on experiments with adhesive strips having a Mylar® or bi-oriented polypropylene (BOPP) backing. The strips were 25.4 mm wide, 127 mm long, and either 0.051 mm, 0.127 mm, or 0.254 mm thick. The substrate was stainless steel, and the contact length was 25.4 mm. Rates of 12 mm/min and 310 mm/min were applied. For the thinner loops, the tack curves exhibited a significant plateau and then a sharp peak, but for the largest thickness there was hardly any plateau region. (If the center of the loop was cut before the loop was pulled off the substrate, no sharp peak occurred.) Most of the loops, especially the thinner ones, demonstrated plastic behavior, including a permanent crease at the center of the loop after detachment.

Finally, Tobing and Klein [12] described tests on Mylar loops that were 25.4 mm wide and 152 mm long. The loops had a backing

thickness of 0.05 mm and the adhesive thickness was 0.025 mm. The rate was 305 mm/min, and values of the tack force were given.

A finite element analysis of the loop tack test was discussed in Hu *et al.* [6], Duncan and Lay [7], and Duncan *et al.* [9]. The program ABAQUS was applied, and a two-dimensional analysis was performed using beam elements. The loop was assumed to be elastic. A simple contact model was adopted and the rheological properties of the adhesive were not included. The effects of the loop thickness and stiffness on the tack force were examined.

An analytical description was presented in Williams [13] and Plaut *et al.* [14]. The adhesive was assumed to be attached to the substrate rather than the loop; this is done in one modification of the loop tack test [2] and used in one of the standard British loop tack tests [7, 8], and also is the situation in probe tack tests [15]. The loop was modeled as an inextensible elastica, but with a nonlinear moment–curvature relation, and the adhesive was treated as a linearly elastic foundation which debonded when extended to a critical value; this value was assumed to depend on the maximum contact pressure and sometimes on the contact time. The results did not correspond to experimentally observed features just before separation of the loop from the substrate; *i.e.*, the tack curves did not exhibit a sharp peak and the loop shapes did not demonstrate high curvatures at the edges of the contact region.

The present study includes an effort to improve that model of the loop tack test and also reports some experimental results. In the finite element analysis, two-dimensional beam elements are used. The loop is assumed to obey an elastic–plastic constitutive law, and high localized curvatures appear before separation of the loop from the substrate. For most cases, the adhesive is modeled with a nonlinearly elastic constitutive law in compression and with a trapezoidal force-separation law in tension (a cohesive zone model [16–19]). Viscoelasticity in the adhesive is considered in one final case.

The experimental work is described in the next section. In the following section, the numerical analysis is presented, and a parametric study is given in the section "Parametric Study". Conclusions are discussed in the last section.

EXPERIMENTAL WORK

In the experiments, the loop was constructed from a strip of stainless steel (Type 300) and was 280 mm long, 12.7 mm wide, and either 0.025 mm, 0.051 mm, 0.076 mm, or 0.102 mm thick. The top of the loop was clamped in an Instron tensile testing machine (Instron,

Canton, MA, USA). 3M^{TM} VHB^{TM} 4950 double-coated acrylic foam tape (3M Co., St. Paul, MN, USA) was placed on the horizontal platform under the loop. The thickness of the PSA was $h_a = 1.14$ mm. The relative vertical displacement of the top of the loop and the platform was decreased at a rate of 12 mm/min. As soon as the contact length reached 25.4 mm, the relative displacement was increased at the same rate. The relative displacement and the force P at the top of the loop were measured until the loop separated from the adhesive. Figure 1 illustrates the shape of the loop at the end of the pushing phase (decreasing relative displacement) and three configurations during the pulling phase (increasing relative displacement).

As shown in Figure 2, the vertical displacement of the top of the loop is denoted y_{top} (positive if upward) and the initial height is $h_{initial} = 119$ mm. Experimental tack curves for loop thicknesses of 0.025 mm and 0.102 mm are shown in Figures 3a and 3b, respectively. Results for the other cases are given in Woo [20]. Initially, the loop is pushed downward, so that P and y_{top} decrease from the origin. When pulling begins, the force-displacement curve essentially follows the pushing curve for a while, and then the adhesive begins to resist and the force increases significantly. Both Figures 3a and 3b exhibit a sharp peak in the force just before separation, and the case with higher thickness contains a distinctive plateau region prior to that. After each test, plasticity effects were noted in the bottom regions of the loops, especially the thinner ones.

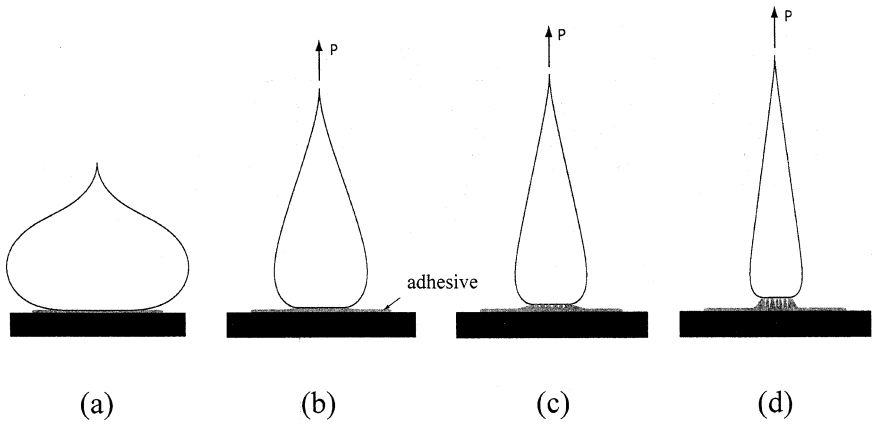

FIGURE 1 Illustration of (a) loop in contact with substrate, (b) to (d) stages in pulling loop off foundation.

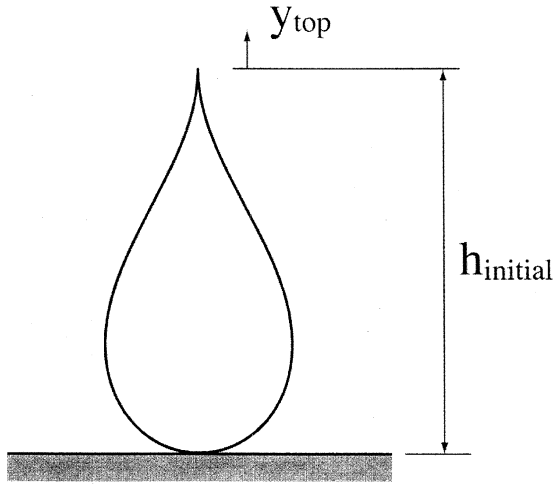

FIGURE 2 Illustration of loop when it comes into contact with substrate.

For each loop thickness, five or six loops were tested. The average values of the tack forces obtained for $h_{loop} = 0.0254$ mm, 0.051 mm, 0.076 mm, and 0.102 mm, respectively, were 8.6 N, 16.7 N, 36.3 N, and 19.9 N. The corresponding coefficients of variation were 0.05, 0.16, 0.23, and 0.10. As the thickness was increased, the tack force

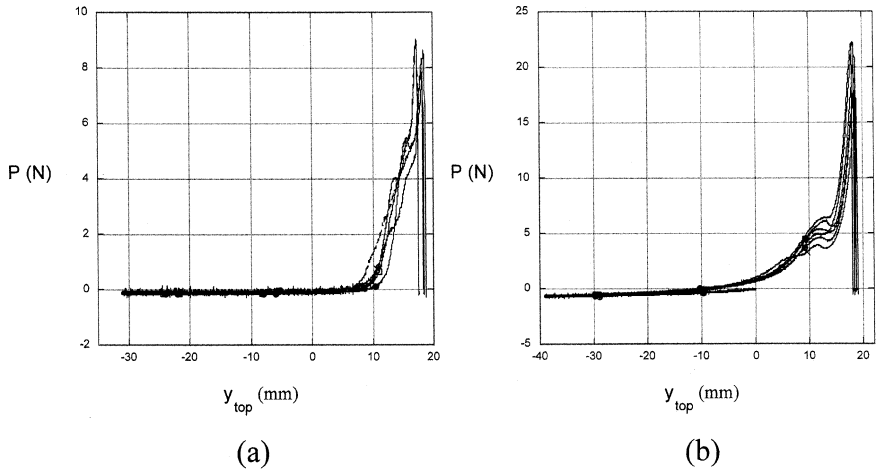

FIGURE 3 Experimental tack curves for (a) $h_{loop} = 0.0254$ mm and (b) $h_{loop} = 0.1016$ mm.

increased except for the last case. Experimental results for the related problem of peeling tape from a rigid surface sometimes demonstrate this nonmonotonic behavior and sometimes are monotonically increasing [21].

NUMERICAL ANALYSIS

The finite element program ABAQUS [22] was utilized to model the behavior observed in the experiments. A three-dimensional simulation was adopted first, using S4R shell elements. Due to symmetry, one-quarter of the loop was modeled [20]. The strip was assumed to be unstrained when straight, and was bent into the loop shape using appropriate applied displacements. It exhibited a small anticlastic curvature (*i.e.*, curvature in the cross-section from one edge to the other, perpendicular to the loop shape in Figure 2), as is also seen in experiments and finite element analyses described in Qi *et al*. [23] in which the ends of the strip were separated by a fixed distance. Three-dimensional effects during the pushing and pulling phases were not very significant (*e.g.*, stresses and displacements were almost constant in each cross section), and the program was very time consuming. Therefore, a two-dimensional formulation was used to obtain the results that are presented here.

Half of the loop is analyzed due to symmetry. It is modeled by 90 B21H hybrid beam elements, with a gradually finer mesh moving away from the clamped (top) end [20]. After the straight strip is transformed into the half-loop shape, the vertical displacement of the clamped end is manipulated incrementally to simulate the pushing and pulling phases of the test. A typical stress-strain result from a tensile test on a steel strip used in the experiments is depicted by the solid curve in Figure 4(a). This is approximated here in ABAQUS as a bilinear elastic–plastic relationship, shown by the dotted line segments for increasing stress.

In most of this study, the adhesive is modeled by nonlinear spring elements (SPRING1) that are initially vertical. The assumed force-displacement relationship is depicted in Figure 4b. When the loop is pushed downward and some springs are compressed, it is assumed that the compressed distance cannot be greater than one-fifth of the adhesive thickness h_a. To model this, the resisting spring force is assumed to approach infinity when this distance is approached, and is assumed to be given by

$$F = E(y_{spring})\frac{y_{spring}}{h_a}A, \tag{1}$$

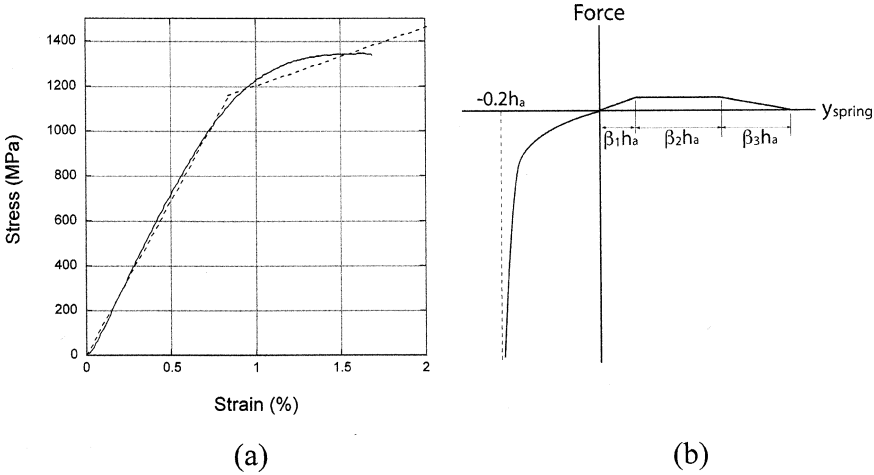

FIGURE 4 (a) Stress *versus* strain for steel loop (experimental and bilinear approximation), and (b) assumed force–displacement relationship for adhesive springs.

where

$$E(y_{spring}) = E_{01}\left[1 + \frac{y_{spring}^4}{\{(0.2h_a)^2 - y_{spring}^2\}^2}\right], \tag{2}$$

E_{01} is the modulus of elasticity at the origin, and A is the tributary area for the node (*i.e.*, the neighboring or effective area).

Figure 4b presents the force *versus* displacement relationship of the nonlinear springs in the compression zone and the tension zone. When a spring is in tension, the trapezoidal relationship shown for positive (upward) spring displacement is shown, involving parameters β_1, β_2, and β_3. (Yang *et al.* [24], analyzing a peel test, also used ABAQUS with a trapezoidal cohesive zone model.) The slope of the force-displacement relationship at the origin in Figure 4b is $E_{01}A/h_a$, so that the maximum tensile spring force is $E_{01}A\beta_1$.

During the incremental procedure, when a node on the strip makes contact with the substrate, the spring at that node becomes active. It remains active during compression and then extension until it is stretched to the value $(\beta_1 + \beta_2 + \beta_3)h_a$.

In the viscoelastic example to be considered, which involves viscoelastic material behavior of the adhesive, a dashpot with viscosity η is added at a node when it first contacts the substrate. It acts parallel to the spring, as in a Kelvin-Voigt model [25]. The dashpot stress is

η times the strain rate, and the dashpot force, f, is given by

$$f = A\,\eta \frac{d\varepsilon}{dt} = A\eta \frac{dy}{dt}\frac{1}{h_a} = c\frac{dy}{dt}, \tag{3}$$

where y is the dashpot displacement (equal to y_{spring}) and $c = A\eta/h_a$. In terms of the constant velocity, v, at the top of the loop, one can write the force at increment $i+1$ as

$$f_{i+1} = cv_{top}\frac{(y_{i+1} - y_i)}{\left|(y_{top})_{i+1} - (y_{top})_i\right|}. \tag{4}$$

The dashpot is active as long as the spring is active.

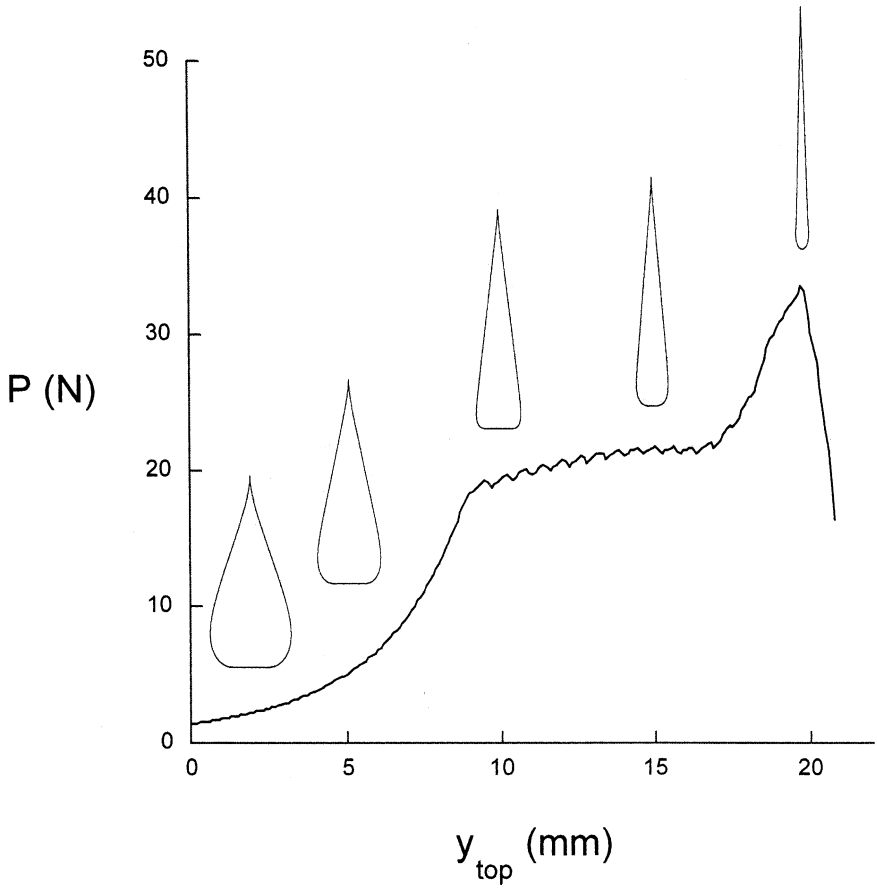

FIGURE 5 Illustration of tack curve for $y_{\text{top}} \geq 0$ and corresponding loop shapes for $y_{\text{top}} =$ 0 mm, 5 mm, 10 mm, 15 mm, and 20 mm.

PARAMETRIC STUDY

In the first set of numerical examples, to match one of the experiments, the loop is 279.4 mm long, 12.7 mm wide, and 0.1016 mm thick, with modulus of elasticity 153 GPa (for the initial deformation) and yield stress 1,109 MPa. The adhesive has thickness $h_a = 1.14$ mm, and its initial modulus of elasticity is taken as $E_{01} = 8$ MPa (obtained from a dynamic mechanical analysis (DMA) test).

Figure 5 depicts a typical tack curve during the pulling phase after $y_{\text{top}} \geq 0$, along with the associated loop shapes occurring at $y_{\text{top}} = 0$ mm, 5 mm, 10 mm, 15 mm, and 20 mm. The plateau region begins when the first spring detaches, and the oscillations that are seen in the tack curve correspond to the detachment of further springs from nodes in the finite element model of the loop during the

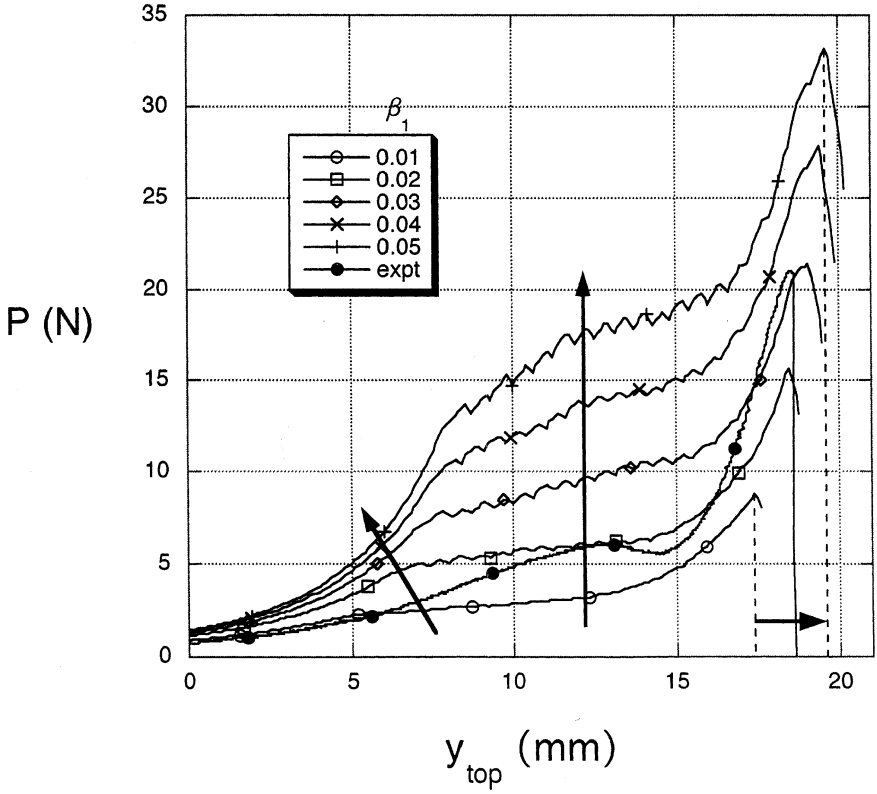

FIGURE 6 Effect of spring parameter, β_1, on tack curve (arrows denote increasing β_1).

incremental numerical procedure. This also occurred in the loop tack study of Hu *et al.* [6] using ABAQUS.

The behavior at the left part of Figure 5 may be similar to that of a peel test. The separation points at the end of the contact region move toward the center of the loop, and fibrils (if fibrillation occurs) resist in an angled direction rather than vertically. As the loop becomes very narrow, the adhesive reacts vertically. This action has more resemblance to a probe tack test in which a stiff flat surface replaces the flexible loop treated here. For probe tests, a sharp peak in the tack curve tends to occur at the beginning of the pulling phase, often followed by a plateau (for a fibrillating adhesive) as the probe detaches from the substrate [15, 26].

The effects of the spring parameters β_1, β_2, and β_3 on the tack curve in the range $y_{top} \geq 0$ during pulling are shown in Figures 6, 7, and 8, respectively. The standard case is taken as $\beta_1 = 0.02$, $\beta_2 = 2$, and

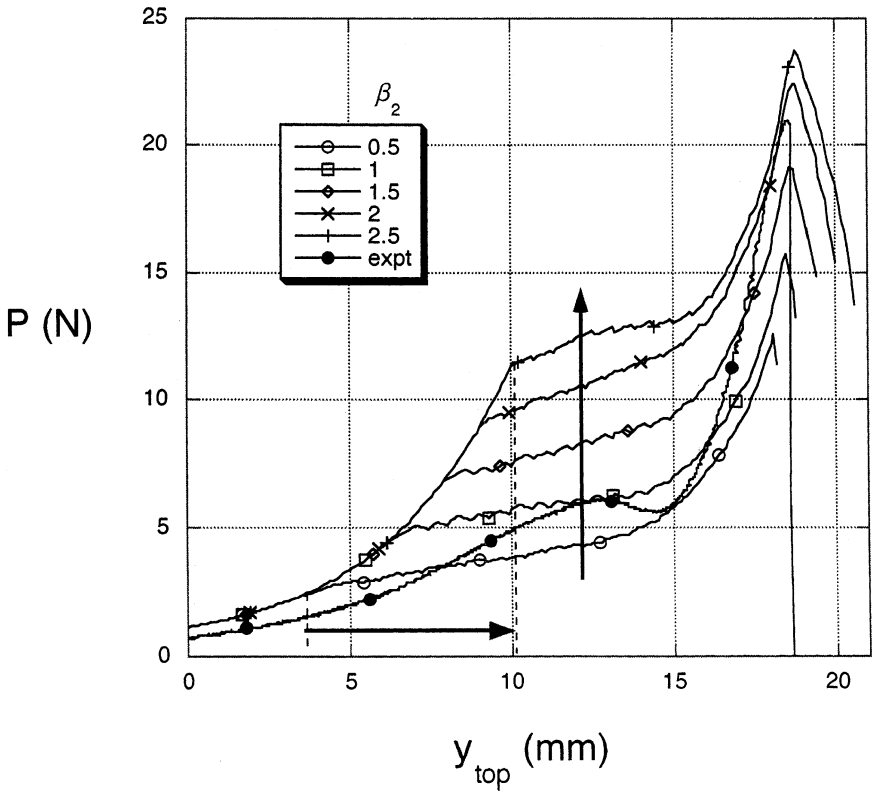

FIGURE 7 Effect of spring parameter, β_2, on tack curve.

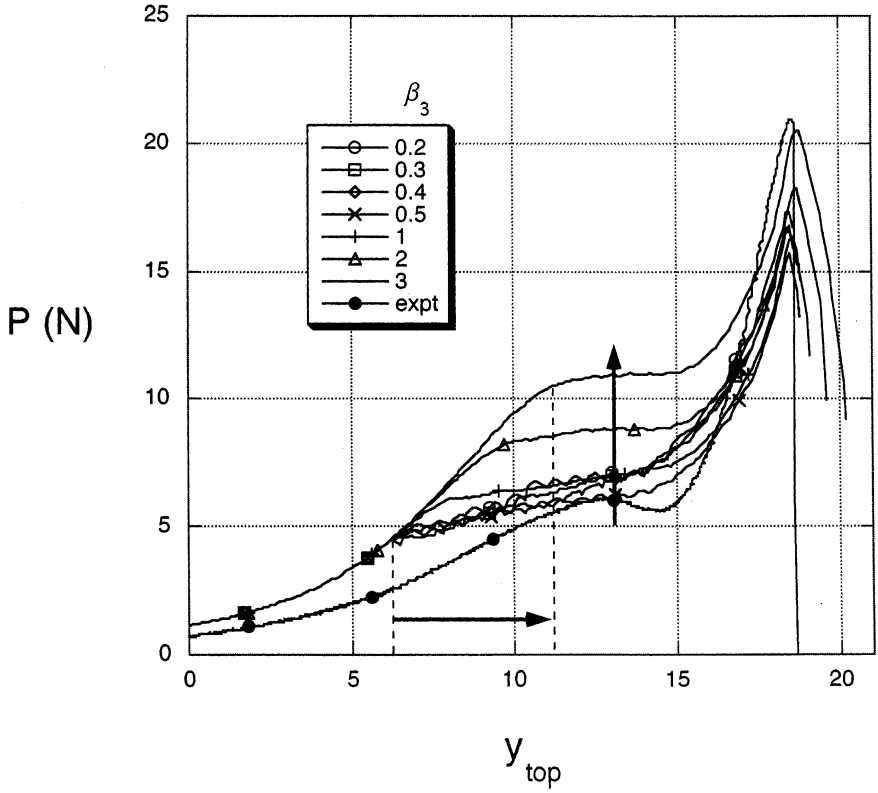

FIGURE 8 Effect of spring parameter, β_3, on tack curve.

$\beta_3 = 0.5$, so the maximum elongation of a spring for this case is $2.52h_a$. The experimental tack curve is denoted by solid circles. Arrows denote the direction of change as the spring parameter of interest is increased.

In Figure 6, β_1 is varied from 0.01 to 0.05, which increases the linearly elastic portion of the traction–separation relationship in Figure 4b. This causes slight increases in the maximum spring elongation (from $2.51h_a$ to $2.55h_a$) and maximum spring tensile force. The initial slope in Figure 6 increases, the force increases and, correspondingly, the final shape of the loop (before detachment) becomes thinner. The tack force increases almost linearly with β_1, and has the values 8.8 N, 15.7 N, 21.4 N, 27.8 N, and 33.2 N, respectively, for $\beta_1 = 0.01$, 0.02, 0.03, 0.04, and 0.05. Sometimes the area under the tack curve, rather than the maximum force, is used as a measure of tackiness; this area is computed for various cases in Woo [20].

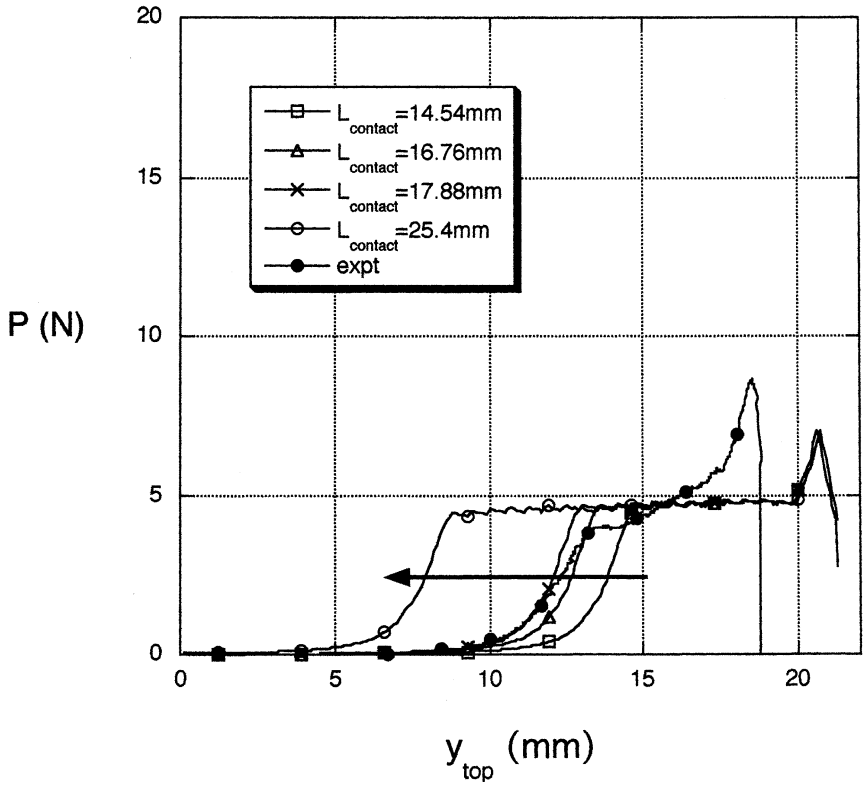

FIGURE 9 Effect of contact length on tack curve.

The parameter β_2 specifies the length of the horizontal (plastic) portion of the constitutive law in Figure 4b. In Figure 7, β_2 is increased from 0.5 to 2.5, with corresponding increase of the maximum spring elongation from $1.02h_a$ to $3.02h_a$ but no change in the maximum tensile spring force. Associated with this, there are increases in the force and the top displacement at which the plateau begins, but little change in the top displacement corresponding to the peak force. However, if the incomplete curves on the right of the peak force are continued downward, one sees that the top displacement at which the loop detaches does increase as β_2 increases. The tack forces for $\beta_2 = 0.5$, 1, 1.5, 2, and 2.5 are 12.6 N, 15.7 N, 19.1 N, 22.5 N, and 23.8 N, respectively, and it increases almost linearly till the last value (as the area of the traction–separation relationship increases).

Finally, the parameter β_3 governs the length of the falling segment in Figure 4b. The value of β_3 is increased from 0.2 to 3 in Figure 8,

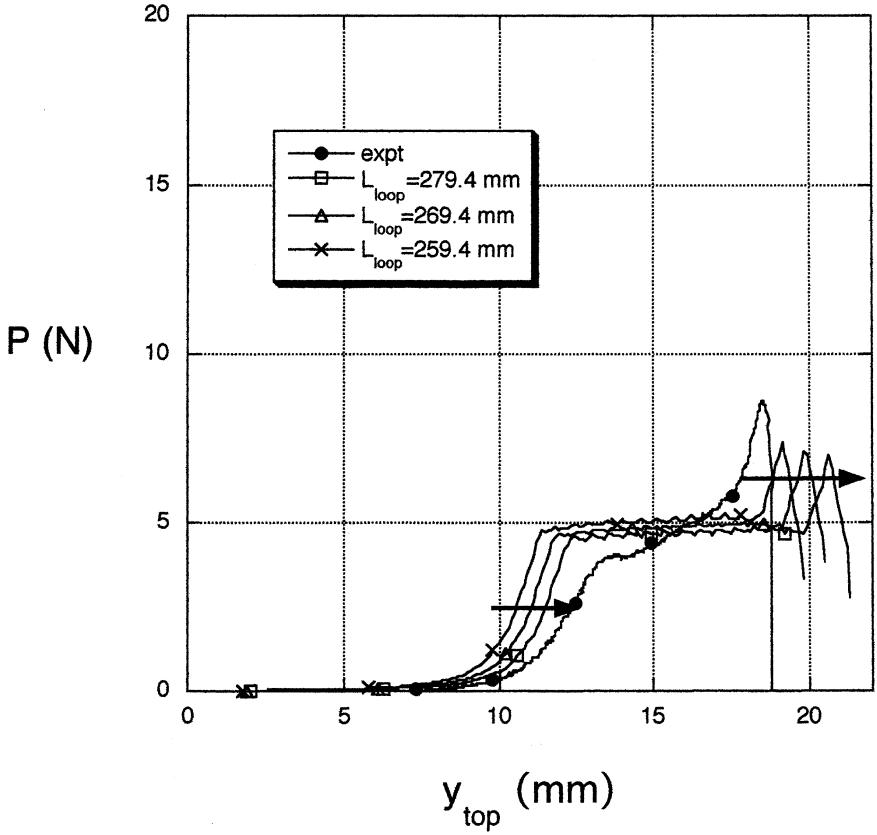

FIGURE 10 Effect of loop length on tack curve.

with the maximum spring elongation changing from $2.22h_a$ to $5.02h_a$, but the maximum tensile spring force remains constant. In Figure 8, the initiation of the plateau region begins at a higher elongation, the length of the plateau region decreases, and the force increases. The tack force has the values 17.3 N, 16.8 N, 16.6 N, 15.7 N, 16.4 N, 18.3 N, and 20.6 N, respectively, for $\beta_3 = 0.2$, 0.3, 0.4, 0.5, 1, 2, and 3. Therefore, for the values of β_1 and β_2 used here, the tack force decreases and then increases as β_3 is increased in this range.

Next, the effect of the contact length at the beginning of the pulling phase is considered. In this case, $h_{\text{loop}} = 0.0254$ mm, the spring parameter β_2 is 0.75, and all other parameters are the same as in the standard case. Figure 9 shows one of the experimental tack curves and computed curves with four different contact lengths. The tack

force is the same for the four numerical solutions. Increasing the contact length causes the length of the plateau region to increase, since more springs become active and then resist debonding according to Figure 4b.

The effect of changes in the length of the loop is depicted in Figure 10. The loop thickness, contact length, and spring parameters are the same as for Figure 9. Along with the standard length of 279.4 mm, shorter lengths of 269.4 mm and 259.4 mm are considered. As the loop length increases, the tack force decreases slightly and the tack curve moves toward the right (as expected, since a longer strip should exhibit larger displacements).

In Figure 11, the thickness of the loop is varied. The spring parameters are the same as for Figures 9 and 10, and the contact length

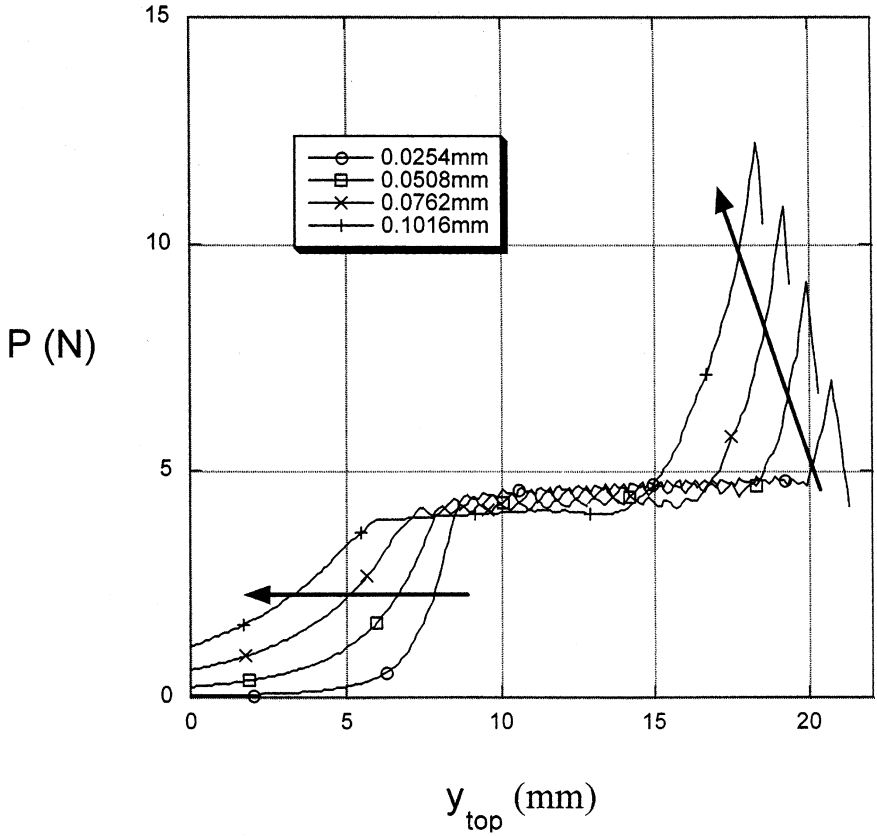

FIGURE 11 Effect of loop thickness on tack curve.

is 25.4 mm. For $h_{\text{loop}} = 0.0254$ mm, 0.0508 mm, 0.0762 mm, and 0.1016 mm, respectively, the tack forces are 7.0, 9.2, 10.9, and 12.3 N. The loop curves move to the left as the maximum force increases. That is, as the loop thickness increases, the loop becomes more resistant to deformation, leading to a greater required tack force and smaller displacements.

The effect of the initial modulus of elasticity, E_{01}, of the adhesive springs (see Equation (2)) is examined in Figure 12. Here $h_{\text{loop}} = 0.1016$ mm, $\beta_1 = 0.02$, $\beta_2 = 1$, and $\beta_3 = 0.2$. Numerical results are presented for $E_{01} = 4$ MPa, 8 MPa (the standard case), 15 MPa, 20 MPa, 50 MPa, and 70 MPa. The corresponding values of the tack force are 9.0 N, 13 N, 20 N, 26 N, 56 N, and 77 N. The tack force increases almost linearly with E_{01} in these results. In the plateau

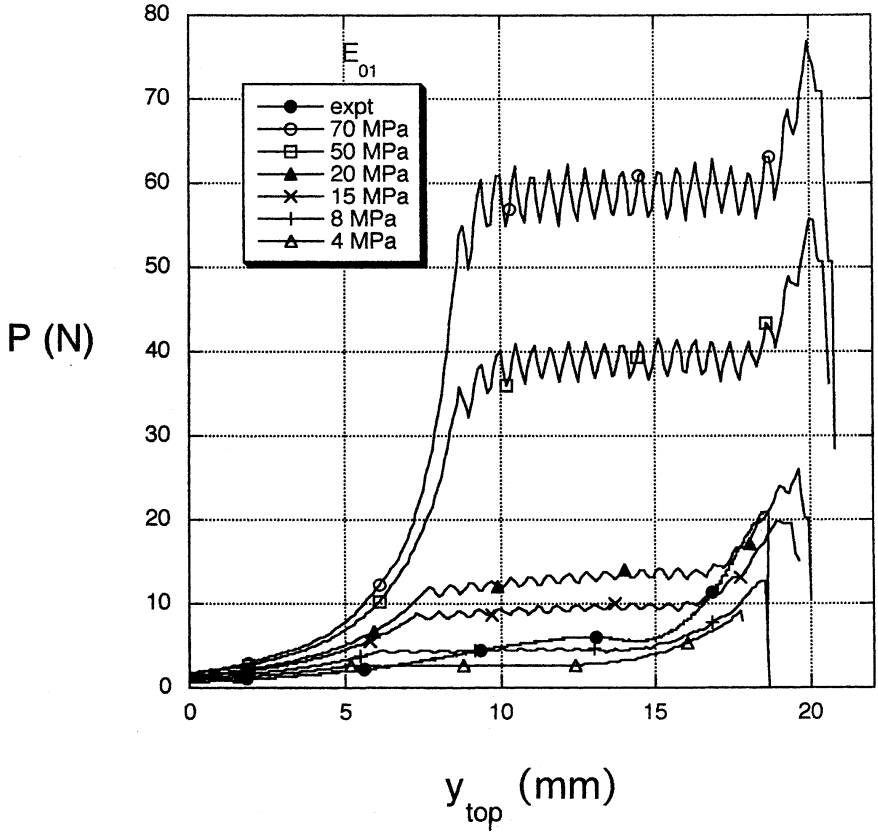

FIGURE 12 Effect of initial adhesive modulus of elasticity on tack curve.

region, the numerical oscillations (as springs detach) become larger as the force increases.

Finally, the viscoelastic model is utilized, using Equations (3) and (4), and results are shown in Figure 13. The pushing and pulling rate, v, at the top of the loop is increased from the value 12 mm/min (as used in the experiments) to 50 mm/min, 100 mm/min, 200 mm/min, and 300 mm/min. The case of no dashpot also is plotted. In these numerical results, $h_{\text{loop}} = 0.1016$ mm, $E_{01} = 8$ MPa, the viscosity, η, of the dashpot is 0.159 MPa-sec (based on DMA tests [20]), and the spring parameters are $\beta_1 = 0.03$, $\beta_2 = 1.5$, and $\beta_3 = 0.2$. The iteration process is described in Woo [20]. For the increasing rates that are utilized, the tack force is 22 N (as for the elastic case), 23 N, 29 N,

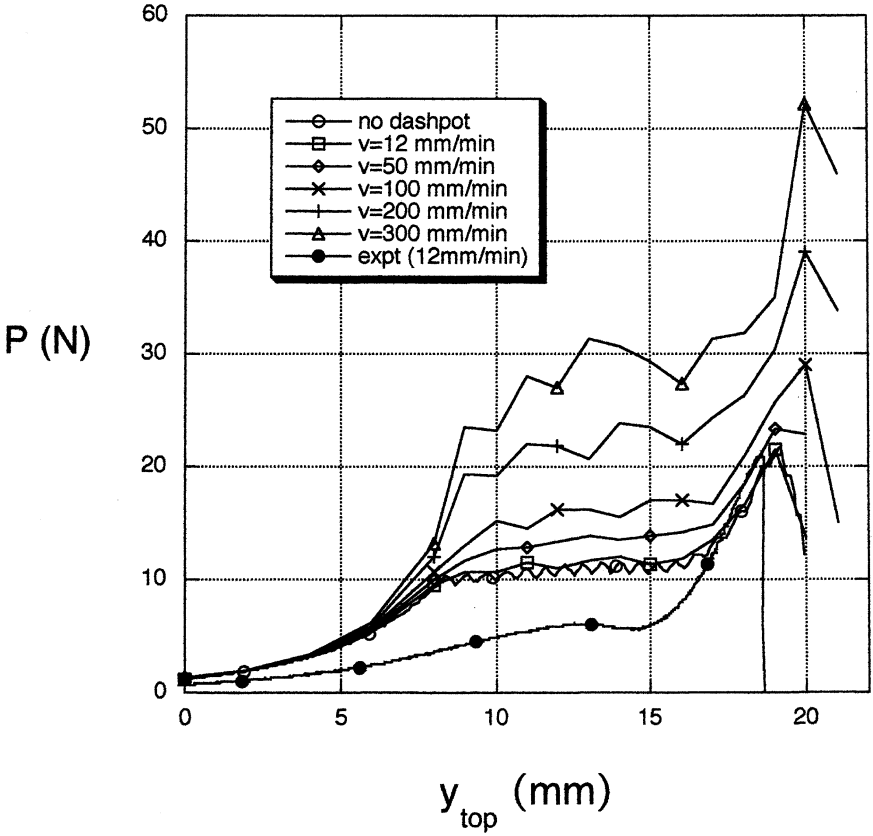

FIGURE 13 Effect of displacement rate (at top of loop) on tack curve.

39 N, and 52 N, respectively (*i.e.*, in these results, the tack force increases as the pulling rate increases).

CONCLUDING REMARKS

The modified form of the loop tack test was considered in which the adhesive is on the substrate rather than on the loop. Experimental results with a steel strip and VHB adhesive were presented. Then a finite element analysis was conducted. Results based a two-dimensional formulation with beam elements were presented. A bilinear elastic–plastic behavior was assumed for the loop. The adhesive was modeled by individual springs, which exhibit a hardening constitutive law in compression, and in tension were governed by a trapezoidal cohesive zone traction–separation law. The springs can be envisaged as fibrils that form during the detachment process [27, 28].

During pulling of the loop, the tack curves (force *versus* displacement) obtained here are comprised of three regions: an initial transition region as the loop begins to elongate; a plateau region as the springs at the edges of the contact region stretch, yield, and detach; and a peak when the loop is very narrow (and the behavior seems to resemble the beginning of a probe tack test). For these loop tack test results, the tack curves have the reverse appearance from those that are typically seen with a probe tack test. Here the peak is at the end of the test rather than at the beginning.

Variations of the spring parameters (β_1, β_2, and β_3) cause significant changes in the tack force (*i.e.*, the maximum force experienced during pulling). The tack curve is very dependent on the assumed total length $(\beta_1 + \beta_2 + \beta_3)\mathrm{h_a}$ of the springs at debonding. A change in the contact area of the loop with the substrate at the beginning of the pulling phase has little effect on the tack force. Small increases in the length of the loop cause the tack force to decrease slightly. Increases in the loop thickness, the initial modulus of elasticity of the adhesive, and the rate of pulling the loop off the substrate cause the tack force to increase in the numerical results. However, in the experiments, as the loop thickness was increased, the tack force initially increased and then decreased.

In a previous study [13, 14], the loop and adhesive were assumed to be linearly elastic. The resulting tack curves did not resemble those obtained from experiments. In particular, they did not exhibit a sharp peak before detachment of the loop from the substrate. In the present numerical analysis, inclusion of elastic–plastic behavior of the loop and the cohesive zone model for the adhesive have produced tack curves exhibiting the main features from the experimental results.

This type of model should be useful for the analysis of loop tack tests involving other loop and adhesive materials, whether the adhesive is on the loop or the substrate.

REFERENCES

[1] Everaerts, A. I., and Clemens, L. M., in *Surfaces, Chemistry & Applications*, Chaudhury, M., and Pocius, A. V. (Eds.) (Elsevier, Amsterdam, 2002), pp. 465–534.
[2] Muny, R. P., *Adhesives Age* **39**(9), 20–24 (1996).
[3] Lin, S. B., *J. Adhesion Sci. Technol.* **10**, 559–571 (1996).
[4] Chuang, H. K., Chiu, C., and Paniagua, R., *Adhesives Age* **40**(10), 18–23 (1997).
[5] Roberts, R. A., *Report No. 5*, Project PAJ1 (National Physical Laboratory, Teddington, UK, 1997).
[6] Hu, F., Olusanya, A., Lay, L. A., Urquhart, J., and Crocker, L., *Report No. 8*, Project PAJ1 (National Physical Laboratory, Teddington, UK, 1998).
[7] Duncan, B. C., and Lay, L. A., *Report No. 11*, Project PAJ1 (National Physical Laboratory, Teddington, UK, 1999).
[8] Duncan, B. C., Abbott, S., and Roberts R., *Measurement Good Practice Guide No. 26*, Project PAJ1 (National Physical Laboratory, Teddington, UK, 1999).
[9] Duncan, B. C., Lay, L. A., Olusanya, A., Roberts, R. A., and Abbott, S. G., *Adhesion '99: Proc. Seventh Int. Conf. on Adhesion and Adhesives*, Cambridge, UK, 1999), Maney Publishing, London, UK, pp. 313–318.
[10] Le, M. N., Qi, J., Dillard, D. A., and Dillard, J. G., *Research Report* (Virginia Polytechnic Institute and State University, Blacksburg, VA, 1999).
[11] Roberts, R. A., *Report No. 10*, Project PAJ1 (National Physical Laboratory, Teddington, UK, 1999).
[12] Tobing, S. D., and Klein, A., *J. Appl. Polym. Sci.* **76**, 1965–1976 (2000).
[13] Williams, N. L., MS Thesis, Virginia Polytechnic Institute and State University, Blacksburg, VA, USA, 2000. Online: http://scholar.lib.vt.edu/theses/available/etd-07132000-14580030
[14] Plaut, R. H., Williams, N. L., and Dillard, D. A., *J. Adhesion* **76**, 37–53 (2001).
[15] Creton, C., and Fabre, P., in *The Mechanics of Adhesion*, Dillard, D. A., and Pocius, A. V. (Eds.) (Elsevier, Amsterdam, 2002), pp. 535–575.
[16] Wei, Y., and Hutchinson, J. W., *Int. J. Fract.* **93**, 315–333 (1998).
[17] Williams, J. G., and Hadavinia, H., *J. Mech. Phys. Solids* **50**, 809–825 (2002).
[18] Georgiou, I., Hadavinia, H., Ivankovic, A., Kinloch, A. J., Tropsa, V., and Williams, J. G., *J. Adhesion* **79**, 239–265 (2003).
[19] Thouless, M. D., and Yang, Q. D., in *The Mechanics of Adhesion*, Dillard, D. A., and Pocius, A. V. (Eds.) (Elsevier, Amsterdam, 2002), pp. 235–271.
[20] Woo, Y., PhD Dissertation, Virginia Polytechnic Institute and State University, Blacksburg, VA, USA, 2002. Online: http://scholar.lib.vt.edu/theses/available/etd-10112002-190728
[21] Satas, D., in *Handbook of Pressure Sensitive Adhesive Technology,* Satas, D. 3rd ed., (Ed.) (Satas and Associates, Warwick, Rhode Island, 1999), pp. 62–86.
[22] Hibbitt, H. D., Karlsson, B., and Sorenson, P., *ABAQUS Version 6.1*, Institute of Materials, London, 1999.
[23] Qi, J., Dillard, D. A., Plaut, R. H., and Dillard, J. G., *J. Adhesion* **79**, 559–579 (2003).
[24] Yang, Q. D., Thouless, M. D., and Ward, S. M., *J. Adhesion* **72**, 115–132 (2000).
[25] Chen, Y.-H., and Sheu, J.-T., *Int. J. Numerical Methods Engrg.*, **36**, 1013–1027 (1993).

[26] Creton, C., in *Materials Science and Technology, Vol. 18: Processing of Polymers*, Cahn, R. W., Haasen, P., and Kramer, E. J. (Eds.) (Wiley-VCH, Weinheim, Germany, 1997), pp. 707–741.
[27] Zosel, A., *Int. J. Adhesion Adhesives* **18**, 265–271 (1998).
[28] Lin, Y. Y., Hui, C. Y., and Wang, Y. C., *J. Polym. Sci. B*, **40**, 2277–2291 (2002).